Received: 6 February 2019 | Revised: 29 August 2019 | Accepted: 6 October 2019

DOI: 10.1111/exd.14047

ORIGINAL ARTICLE

Experimental Dermatology WILEY

DNA hypermethylation is associated with invasive phenotype of malignant melanoma

Viktória Koroknai[1,2] | István Szász[1,2] | Hector Hernandez-Vargas[3] | Nora Fernandez-Jimenez[3] | Cyrille Cuenin[3] | Zdenko Herceg[3] | Laura Vízkeleti[1,2] | Róza Ádány[1,2] | Szilvia Ecsedi[1,2,3] | Margit Balázs[1,2]

[1]Public Health Research Institute, University of Debrecen, Debrecen, Hungary

[2]MTA-DE Public Health Research Group, Public Health Research Institute, University of Debrecen, Debrecen, Hungary

[3]Epigenetics Group, International Agency for Research on Cancer (IARC), Lyon, France

Correspondence
Margit Balázs and Szilvia Ecsedi, Public Health Research Institute, University of Debrecen, Debrecen, Kassai str 26. 4028, Hungary.
Emails: balazs.margit@sph.unideb.hu (M. B.); Szilvia.Ecsedi@unice.fr (S. E.)

Funding information
This research was supported by the National Research Development and Innovation Fund (grant numbers K112327), by the ÚNKP-18-3 New National Excellence Programme of the Ministry of Human Capacities (to VK and ISz) and by the IARC Postdoctoral Fellowship and Marie Curie Actions-People-COFUND (to SE). The work was co-financed by the European Union under the European Social Fund and European Regional Development Fund (GINOP-2.3.2-15-2016-00005). The work in the IARC Epigenetics Group is partially supported by grants from EC Eurocanplatform: A European Platform for Translational Cancer Research); the Association pour la Recherche sur le Cancer (ARC), France; and la Ligue Nationale (Française) Contre le Cancer, France (to ZH).

Abstract

Tumor cell invasion is one of the key processes during cancer progression, leading to life-threatening metastatic lesions in melanoma. As methylation of cancer-related genes plays a fundamental role during tumorigenesis and may lead to cellular plasticity which promotes invasion, our aim was to identify novel epigenetic markers on selected invasive melanoma cells. Using Illumina BeadChip assays and Affymetrix Human Gene 1.0 microarrays, we explored the DNA methylation landscape of selected invasive melanoma cells and examined the impact of DNA methylation on gene expression patterns. Our data revealed predominantly hypermethylated genes in the invasive cells affecting the neural crest differentiation pathway and regulation of the actin cytoskeleton. Integrative analysis of the methylation and gene expression profiles resulted in a cohort of hypermethylated genes (*IL12RB2*, *LYPD6B*, *CHL1*, *SLC9A3*, *BAALC*, *FAM213A*, *SORCS1*, *GPR158*, *FBN1* and *ADORA2B*) with decreased expression. On the other hand, hypermethylation in the gene body of the *EGFR* and *RBP4* genes was positively correlated with overexpression of the genes. We identified several methylation changes that can have role during melanoma progression, including hypermethylation of the promoter regions of the *ARHGAP22* and *NAV2* genes that are commonly altered in locally invasive primary melanomas as well as during metastasis. Interestingly, the down-regulation of the methylcytosine dioxygenase *TET2* gene, which regulates DNA methylation, was associated with hypermethylated promoter region of the gene. This can probably lead to the observed global hypermethylation pattern of invasive cells and might be one of the key changes during the development of malignant melanoma cells.

KEYWORDS
cell invasion, DNA methylation, gene body, malignant melanoma, TET2

Szilvia Ecsedi and Margit Balázs authors contributed equally to this work.

1 | INTRODUCTION

Melanoma is a neural crest-derived tumor that develops from melanocytes originating from a highly migratory embryonic cell population.[1–3] The mechanism of migration and invasion, key processes of cancer cell progression which leads to life-threatening metastatic tumors, is poorly understood.[4–6]

According to recent studies, the cellular plasticity that promotes invasion strategies in malignant melanoma is mainly due to environmental stimuli and is accompanied by transcriptomic reprogramming.[7]

Based on a recent study by Verfaillie et al,[7] the proliferative and invasive transcriptomic signatures are highly correlated with permissive and repressive chromatin states underlining the importance of epigenetic regulation in the acquisition of the invasive cellular state. Indeed, the expression of the MITF and SOX10 transcription factors, which are master regulators of the proliferative gene network, has been confirmed. In the contrary, invasive cells exhibit high expression levels of *TEAD* and *AP1* genes.[8,9]

Due to the lack of direct genetic components in transcriptional reprogramming, studying the epigenetic factors that may promote cellular plasticity leading to increased invasion and metastasis is reasonable.[10] Based on the Cancer Genome Atlas Network (TCGA), the well-established mutational classifications of melanomas are not in agreement with gene expression patterns, which could explain not only the low response rate of therapies targeting the aforementioned mutations but also the concerns raised against the durability of such interventions.[11] Nevertheless, the strong association between the mutations of chromatin remodelling genes (ARID2 and IDH1) and the high degree of DNA methylation at several promoter regions described in melanoma (CpG island methylator phenotype; CIMP) suggests that epigenetic factors might play a pivotal role in cellular plasticity leading to increased invasion and metastasis.[11,12]

Epigenome-wide (EWAS) DNA methylation studies implemented during the last few years have greatly improved our understanding on the importance of CIMP in the silencing of tumor suppressor and developmental genes. Several genes of the melanocyte lineage differentiation pathway were found to be methylated such as KIT, PAX3, SOX10, different members of the HOX family genes and MITF.[13–16] Remarkably, comparing matched primary and metastatic melanoma cell lines, Chatterjee et al[17] found EBF3 promoter hypermethylation as a possible epigenetic driver of melanoma metastasis.

Importantly, EWAS on melanomas have more often focused on the metastatic tumors, and therefore, the DNA methylation changes accompanying the early molecular invasion events remain to be elucidated. Only a single study used cell lines derived from primary melanomas, and the authors applied melanocytic markers to distinguish between invasive and less invasive cell lines and found that SOX9 demethylation is associated with melanoma cell invasion and metastasis and decreases patient survival.[18]

There is a great need of identifying early metastasis-promoting epigenetic events, and our main goal was to study the DNA methylation landscape of early invasion using a direct, in vitro selection for the invasive melanoma subpopulation derived from primary malignant melanomas.

2 | MATERIALS AND METHODS

2.1 | Cell culture

Experiments were performed in primary tumor-derived melanoma cell lines WM983A (Coriell Cat# WC00048, RRID:CVCL_6808), WM793B (Coriell Cat# WC00062, RRID:CVCL_8787), WM1366 (Coriell Cat# WC00078, RRID:CVCL_6789) and WM3211, (Coriell Cat# WC00045, RRID:CVCL_6797). The cells were cultured in RPMI 1640 medium (Lonza Group Ltd.) supplemented with 10% foetal bovine serum (Gibco) at 37°C in 5% CO_2.

2.2 | In vitro invasion assay and selection

The invasive potential of melanoma cell lines was analysed using BD Biocoat Matrigel invasion chambers (pore size: 8 μm, 24-well; BD Biosciences). The upper chamber of the insert was filled with 500 μL of cell suspension in serum-free media (5×10^4 cells/well). Medium containing 10% FBS was added to the lower chamber as a chemoattractant. After the cells were incubated for 24 hours at 37°C, cells in the lower layer were fixed with methanol and stained with haematoxylin-eosin. The invading cells were counted in seven different visual fields under a light microscope at ×200 magnification, and the data are presented as the means ± SD of three independent experiments. To select the invasive subpopulations, the invading cells in the lower layer chamber were treated with 0.5% trypsin/0.2% EDTA (Sigma-Aldrich Inc) for recovery from the membrane and cultured using standard protocols. The selected subpopulations were designated WM983A-INV, WM793B-INV, WM1366-INV and WM3211-INV. DNA and RNA were isolated from invasive subpopulations of each sample. The invasive potential of the selected invasive subpopulation was measured in parallel with nucleic acid isolations.

2.3 | Cell proliferation assay

Cell proliferation rate was determined using the WST-1 assay (Sigma-Aldrich Inc) according to the manufacturer's guidelines. Briefly, cells were seeded in 96-well in triplicate and cultured for 24, 48, 72 and 96 hours. Then, 10 μL of WST-1 was added directly to the culture medium in each well, and the cells were incubated for another 3 hours. Absorbance was measured at 450 nm using a NanoDrop UV-Vis spectrophotometer (RRID:SCR_016517; NanoDrop Technologies). The reference absorbance was set at 700 nm.

2.4 | Genome-wide DNA methylation analysis

DNA was extracted using a standard procedure of the G-spin Genomic DNA extraction kit (Intron Biotechnology Inc). DNA quantification was done NanoDrop. For methylation studies, bisulphite modification was performed on 600 ng of DNA using EZ DNA Methylation

kit (Zymo Research). The quality of modification was confirmed by PCR (HotStarTaq Master Mix kit; Qiagen GmbH) using modified and unmodified primers for the *GAPDH* gene. The DNA methylome profiling was performed using an Illumina Infinium Human Methylation 450K (HM450K) BeadChip assay (Illumina), which includes more than 480 000 methylation sites.[19] The array experiments were performed by the Epigenetics Group and the Core Facility of the Genetic Cancer Susceptibility Group, International Agency for Research on Cancer. The raw data were deposited in the Gene Expression Omnibus (GEO) repository (http://www.ncbi.nlm.nih.gov/gds, RRID:SCR_005012) under accession number GSE115852.

The data preprocessing and all analyses were performed using several Bioconductor packages in R v.3.2.2 (http://www.r-project.org/, RRID:SCR_001905) as described before.[20–29] See the deadline pipeline of the bioinformatical analysis in the Methods S1. In brief, raw methylation data were imported and processed using the "Lumi v2.36.0," "wateRmelon v1.28" and "minfi v1.30" packages.[20–22] Probes were filtered for low quality with the "pfilter" function, and additionally, known cross-reactive probes were also excluded from further analysis.[21,23] The remaining data set was background-subtracted and normalized using intra-array beta-mixture quantile normalization.[24] Methylation beta values were logarithmically transformed to M values before parametric statistical analyses, as recommended.[25] To define differentially methylated positions (DMPs) and differentially methylated regions (DMRs), first, we modelled the main variables (invasive capacity) as a categorical variable in a linear regression using the "limma v3.40.2" package an empirical Bayesian approach.[26] To infer the detected differentially methylated sites into DMRs, we used the "DMRcate v1.20" package with the recommended proximity-based criteria: if a region harboured at least 3 probes spanning in 1 kb.[27] For the annotations, to obtain information of the nearest gene and transcript of each the detected DMR, we used the FDb.InfiniumMethylation.hg19 v.2.2.0 package, using hg19 as a reference genome.[28] For the visualizations, we used either the DMRcate or the coMET packages with the functionality of the Gviz package.[30]

2.5 | Correlation between gene expression and DNA methylation

RNA was isolated using RNeasy Plus Mini Kit (Qiagen GmbH) and then assessed using NanoDrop and Bioanalyzer (Agilent Technologies). To assess gene expression at genome-wide levels, we purchased Affymetrix Human Gene 1.0 microarrays (Affymetrix Inc). The labelling, hybridization and imaging setup were performed in UD-GenoMedMedical Genomic Technologies Ltd. (University of Debrecen, Clinical Genomic Center) using 500 ng of sample RNA. The raw CEL files were imported to R v.3.2.2 using the Oligo package. The filtering and normalization were performed using the Minfi and WateRmelon packages. We calculated Pearson's correlation coefficients to correlate the gene expression $\log_2$ fold changes in the DNA methylation changes ($\Delta\beta$) in the genes belonging to the DMPs. The microarray data are available in the GEO (http://www.ncbi.nlm.nih.gov/gds, RRID:SCR_005012) under accession number GSE114380.

2.6 | TCGA-SKCM data analysis

We downloaded Illumina Methylation 450K data available for SKCM from the TCGA-GDC data portal (https://portal.gdc.cancer.gov/) by using the GDCquery and GDCprepare functions of the TCGAbiolinks R package.[31] The latter generated a summarized experiment object that we further analysed by using the TCGAanalyze_DMR function of the TCGAbiolinks package with a mean delta-beta cut-off 10% and a Benjamini-Hochberg adjusted *P*-value of .05. The rest of the settings were the default options recommended by the developers of the package. We compared the tumors classified as "metastatic" vs "primary" according to the definition column of the clinical data available at the data portal. Afterwards, we added a variable to the colData data frame of the summarized experiment by using the addAnnotation function of the IntEREst R package,[32] consisting of a merge of any Clark level below stage V into a single category to compare primary tumors by invasiveness (V vs not-V), and finally rerun the TCGAanalyze_DMR function as described above.

2.7 | Real-time quantitative PCR analysis

The relative expression level of 20 genes that are related to methylation (*DNMT1*, *DNMT3A*, *DNMT3B*, *TET1*, *TET2*, *UHRF1* and *UHRF2*), neural crest differentiation (*MITF*, *PAX6*, *PMEL*, and *RHOB*) and cell invasion property (*LEF1*, *NNMT*, *EDNRB*, *TERC*, *CDH13*, *HCK*, *ST8SIA1*, *EGFR* and *ID4*) was determined by quantitative real-time PCR using a LightCycler 480 Real-Time PCR System (Roche Diagnostics GmbH) as previously described.[33] The primer sequences are listed in Table S1.

3 | RESULTS

3.1 | Phenotypic characterization of selected invasive cells

To identify the invasion-related gene expression changes and genome-wide DNA methylation patterns in melanoma cells, invasive cell subpopulations were selected from the original cell lines (WM983A, WM1366, WM3211 and WM793B) using Matrigel-coated invasion chambers. In this way, we establish selected invasive cell populations (WM983A-INV, WM1366-INV, WM3211-INV and WM793B-INV). Afterwards, the invasion potential and the proliferation rate of the selected invasive cells were compared with the original cell lines. We found that three of the selected cell lines (WM1366-INV, WM793B-INV and WM983A-INV) had significantly higher invasive potential compared with the original cell lines ($P < .05$ by Mann-Whitney test). On the other hand, the proliferation rate was lower of the invasive cell lines than the original cell lines, and however, the difference was not statistically significant (Figure 1A and B).

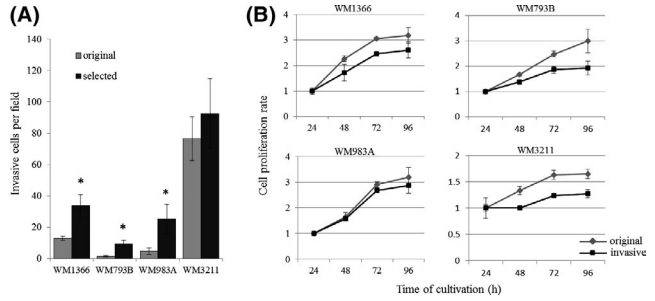

FIGURE 1 Invasive potential (A) and proliferation rate (B) of the original (WM1366, WM793B, WM983A and WM3211) and selected invasive (WM1366-INV, WM793B-INV, WM983A-INV and WM3211-INV) melanoma cell lines. The asterisk indicates statistically significant difference (Mann-Whitney test: $P < .05$). The data are presented as the mean ± SD of three independent experiments

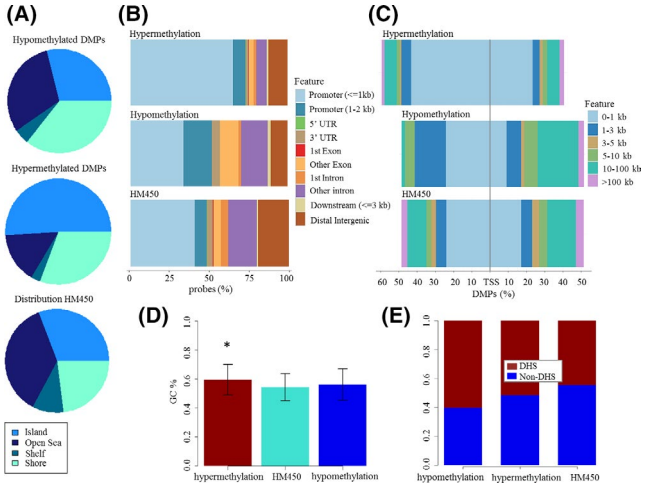

FIGURE 2 Genomic features of differentially methylated regions between the selected invasive and original cell lines. A, The distribution of the DMPs was analysed according to the CpG islands (island, "open sea," shelf and shore). B, DMP position relative to the genes (promoter, UTRs and intron/exon) and (C) distance to transcription start sites (TSSs). D, GC content of hypermethylated and hypomethylated probes. E, DMP positions relative to DNAse I hypersensitivity sites. The total bead array probe distribution (HM450) is shown for all plots as a reference. The results are shown for the hypermethylated and hypomethylated probes. The error bars mark the standard deviations. The asterisk shows statistically significant ($P < .05$)

3.2 | Methylation profile of selected invasive cells

To define the methylation patterns of the cell lines, we used robust methylation profiling platform, which allowed to compare epigenome-wide data of selected invasive melanoma cell subpopulations (WM983A-INV, WM793B-INV, WM1366-INV and WM3211-INV) to the original cell lines (WM983A, WM793B, WM1366 and WM3211). Globally, hypermethylated DMRs (n = 1216) were considerably more prevalent than the hypomethylated DMRs (n = 33) with a total of 8733 and 165 CpG sites, respectively. The full list of hyper- and hypomethylated DMRs and CpG sites are shown in Tables S2 and S3.

As shown in Figure 2A, while the hypermethylated CpG probes (DMPs) exhibited enrichment for CpG islands, the distributions of the hypomethylated DMPs were mostly detected in CpG shores (the 2 kb region upstream and downstream flanking the promoter CpG islands) and open seas (more than 4 kb from the promoter CpG island). Compared with the distribution of all bead array (HM450) probes, the hypermethylated DMPs showed marked increase within the closer promoter regions, within 1 kb distance to their annotated TSS (Figure 2B), while the hypomethylated DMPs were enriched in the distant (1-2 kb) promoter region (Figure 2C). The hypermethylated DMPs were significantly enriched in DNase I hypersensitive sites marking cis-regulatory regions (DHSs) (Figure 2E). Furthermore, we observed significant difference in the GC content between hypermethylated probes and all bead array (HM450) probes (Figure 2D).

We applied more stringent criteria to determine significant DMRs with increased $\Delta\beta_{mean}$ > 10% between the invasive and the original cell lines. As a result, we identified the predominance of hypermethylation as 416 DMRs with 1982 DMPs (corresponding to 384 genes) showed hypermethylation in the selected invasive population, and only one DMR with 3 DMPs (corresponding to one gene) were hypomethylated (Tables S2 and S3). The top significant DMR presented with 15 differentially methylated probes and showing more than 20% $\Delta\beta_{mean}$ was a 1950 bp region that included the *BAALC* gene with its corresponding non-coding RNA (ncRNA) pair, *BAALC-AS2*. Genes as *MITF*, *CYP27A1* and *GRIA2* with well-known functions in melanomas were also present among the significant DMRs.

To define the potential functional changes associated with DNA hypermethylation in invasive melanoma cells, we performed pathway analysis and found that hypermethylation mostly affected the neural crest differentiation pathway (WP2064; (*NOTCH3*, *PAX7*, *HEY2*, *MITF*, *FGFR2*, *FGFR3*, *RHOB*, *MSX2*, *TLX2* and *ZIC5* genes) and the regulation of actin cytoskeleton pathway (WP51; eg, *MOS*, *GSN*, *ACTN1*, *WASF2* and *VAV1* genes; Table S4).

3.3 | Integration of methylation and gene expression profiles

To determine the functional relevance of the DNA methylation changes, we performed integrative analysis of the DNA methylation and gene expression alterations.

We identified a total of 886 significantly correlated CpG sites corresponding to 392 individual genes, of which 220 showed negative, whereas 172 genes exhibited positive correlation between DNA methylation and gene expression (Table S5). Although both the negatively and positively correlated CpGs exhibited enrichment for the closer promoter regions (Figure 3A), the increase was remarkable for differential methylation that exhibited negative correlation with the gene expression. If we compared the negatively correlated CpGs to the Infinium HumanMethylation450 BeadChip probes, we observed an enrichment within 1 kb distance upstream and downstream from the transcription start sites (TSSs) of the corresponding coding genes, while the positively correlated CpGs were enriched in 1-3 kb downstream from the TSSs (Figure 3B).

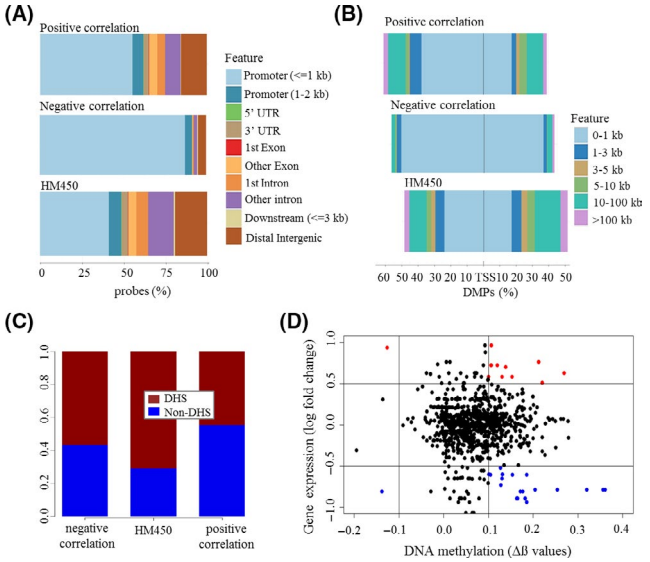

FIGURE 3 Integration of methylation and gene expression profiles related to melanoma invasiveness. A, Positively and negatively correlated probes relative to the genes (promoter, UTRs or intron/exon) and (B) distance to transcription start sites (TSSs). C, Positively and negatively correlated DMP positions relative to DNAse I hypersensitivity sites. D, A starburst plot corresponding to correlation analysis between DNA methylation and gene expression changes. The filtered mean log expression and methylation data are shown in a correlation plot (1-fold expression differences between the invasive and the original cell lines were correlated to DMPs of Δβmean > 10%). Probes with increased gene expression are shown in red, and probes with decreased expression are highlighted in blue

Interestingly, CpG island shore hypermethylation was associated with decreased expression in case of four DMRs corresponding to *RHOB*, *ID4*, *ST8SIA1* and *GRIA2* genes (Figure S1).

For further correlation analysis, we used more stringent criteria: genes with 1-fold expression differences (log2 fold change > ±0.5) between the invasive and the original cell lines were correlated with DMPs of $\Delta\beta_{mean}$ > 10% (Table 1). As shown in Figure 3D, majority of the genes were negatively correlated, that is hypermethylation was associated with decreased gene expression (*IL12RB2*, *LYPD6B*, *CHL1*, *SLC9A3*, *BAALC*, *FAM213A*, *SORCS1*, *GPR158*, *FBN1* and *ADORA2B*; lower right segment, Figure 3D), while a few genes exhibited positive correlation between hypermethylation and increased gene expression (*MCC*, *PTCHD4*, *EGFR*, *RBP4* and *FAR2*; upper right segment, Figure 3D).

Additionally, two hypomethylated genes revealed significant correlation with either up-regulation (*NNMT*; upper left segment; Figure 3D) or down-regulation (*NBPF8*; lower left segment; Figure 3D) of gene expression.

3.4 | Invasion-related methylation changes in melanoma tumor samples

To validate the importance of methylation changes observed in the selected invasive cells, first, we determined and compared our results to the DNA methylation changes present in the TCGA metastatic melanomas (n = 349) vs tissues of primary sites (n = 88). Altogether, 879 genes (corresponding to 1984 differentially methylated regions) exhibited significant differences between the metastatic and primary melanomas of the TCGA cohort (Table S6), from which 28 genes out of our differentially methylated 385 genes showed overlap to the TCGA metastatic melanomas. Remarkably, several of the overlapping genes between the 2 data sets have already well-established role in invasion and metastasis formation, of which includes *TP73*, *HOXD13*, *PAX6*, *ITPKA*, *NR2F2*, *SLC17A7*, *SPTBN1*, *AHNAK*, *CCL23*, *NFE2L3* and *SLC9A*.[14,34] Furthermore, 10 out of the 28 genes seem to have a role in the transcriptomic reprogramming during early invasion: the methylation changes in *CBFA2T3*, *TP73*, *CTSK*, *NAV2*, *PAX6*, *ARHGAP22*, *SDK1*, *ATP11A*, *RASA3* and *SLC9A3* showed significant correlation with gene expression changes.

However, this comparison has the limitation, that is later metastatic events are not necessarily characteristic for those that arise at the early stages of invasion.[35,36] For this reason, we aimed to concentrate on the 88 primary melanoma tissues and used Clark staging as the most relevant clinical parameter to differentiate between locally invasive (Clark stage V; n = 20) and early stage (all Clark stages below V; n = 41) referred as less invasive. We identified 448 differentially methylated genes (corresponding to 1269 probes) seem to have a role during early invasion represented by the Clark staging system (Table S6). Of note, 18 out of the 385 genes in our data set show overlap with the TCGA data, of which several genes (*MECOM*, *CHD5*, *TRIM55*, *FZD6*, *TPBG* and *TRPC4*) were observed in association with invasion.[37–42]

Comparing our data with the TCGA, the most interesting finding is the hypermethylation of *ARHGAP22* and *NAV2* genes that were commonly detected in locally invasive primary melanomas as well as during metastasis.

3.5 | Expression of DNMTs, UHRFs and TETs

To investigate the possible biological background of different methylation patterns between the selected invasive and the original cell lines, we analysed the relative mRNA expression of the DNA methyltransferases (*DNMT1*, *DNMT13A* and *DNMT13B*), the ubiquitin-like protein containing PHD and RING finger domains 1 and 2 (*UHRF1* and *UHRF2*) and the TET methylcytosine dioxygenase enzymes (*TET1* and *TET2*), all playing a crucial role in the maintaining and removing of epigenetic marks. We observed that each of the selected invasive cells had decreased DNMT1 and DNMT3B expressions compared with the original cell lines (Figure 4A). *UHRF1* and *UHRF2* genes also showed down-regulation in invasive cells compared with the original cell lines (Figure 4B). Additionally, the expression levels of TET1 and TET2 were also remarkably lower in two of the four invasive cells (WM983A-INV and WM3211-INV) than in the original cell lines (Figure 4C). Unexpectedly, TET2 down-regulation was associated with hypermethylation at the *TET2* gene promoter region in the invasive subpopulation (Figure 4D).

TABLE 1 Significant correlation between filtered differentially methylated probes (DMPs) and gene expression data

Chr.	Start	End	Nearest gene symbol	Nearest TSS	Mean Δβ	Mean logFC	*P*-value	Correlation coefficient (*R*)
Negative correlation								
chr1	67772986	67772987	*IL12RB2*	*IL12RB2*	0.13	−0.73	1.95E-02	−0.79
chr2	149895023	149895024	*LYPD6B*	*LYPD6B*	0.14	0.70	3.54E-02	−0.74
chr3	238618	238619	*CHL1*	*CHL1*	0.13	−0.65	1.40E-02	−0.81
chr5	497639	497640	*SLC9A3*	*PP7080*	0.13	−0.60	2.07E-02	−0.79
chr5	497397	497398	*SLC9A3*	*PP7080*	0.10	−0.60	4.04E-02	−0.73
chr8	104153592	104153593	*BAALC*	*BAALC*	0.25	−0.79	2.40E-02	−0.77
chr8	104153637	104153638	*BAALC*	*BAALC*	0.32	−0.79	3.42E-02	−0.74
chr8	104153767	104153768	*BAALC*	*BAALC*	0.20	−0.79	2.33E-02	−0.78
chr8	104153627	104153628	*BAALC*	*BAALC*	0.36	−0.79	4.11E-02	−0.73
chr8	104153643	104153644	*BAALC*	*BAALC*	0.36	−0.79	3.02E-02	−0.76
chr10	82167774	82167775	*FAM213A*	*FAM213A*	0.18	−0.89	3.41E-03	−0.89
chr10	82167757	82167758	*FAM213A*	*FAM213A*	0.17	−0.89	2.57E-03	−0.90
chr10	108924867	108924868	*SORCS1*	*SORCS1*	0.19	−0.94	1.64E-02	−0.80
chr10	25464418	25464419	*GPR158*	*GPR158*	0.13	−0.53	3.58E-03	−0.88
chr10	82167764	82167765	*FAM213A*	*FAM213A*	0.16	−0.89	1.38E-03	−0.92
chr11	114165661	114165662	*NNMT*	*NNMT*	−0.13	0.94	4.01E-02	−0.73
chr15	48938576	48938577	*FBN1*	*FBN1*	0.12	0.73	6.12E-03	−0.86
chr15	48938239	48938240	*FBN1*	*FBN1*	0.11	0.73	4.66E-03	−0.87
chr15	48938370	48938371	*FBN1*	*FBN1*	0.11	0.73	3.70E-03	−0.88
chr17	15848264	15848265	*ADORA2B*	*ADORA2B*	0.15	−0.61	3.02E-03	−0.89
chr17	15848828	15848829	*ADORA2B*	*ADORA2B*	0.10	−0.61	2.08E-04	−0.96
chr17	15848253	15848254	*ADORA2B*	*ADORA2B*	0.185	−0.609	6.03E-04	−0.94
Positive correlation								
chr1	147737024	147737025	*NBPF8*	NA	−0.14	−0.81	3.62E-02	0.74
chr5	112824765	112824766	*MCC*	*MCC*	0.21	0.76	1.10E-02	0.83
chr6	48036605	48036606	*PTCHD4*	*PTCHD4*	0.15	0.58	4.16E-02	0.73
chr6	48036409	48036410	*PTCHD4*	*PTCHD4*	0.13	0.58	3.79E-04	0.95
chr6	48036280	48036281	*PTCHD4*	*PTCHD4*	0.10	0.58	5.02E-05	0.97
chr7	54956598	54956599	*EGFR*	*EGFR*	0.27	0.63	1.24E-02	0.82
chr10	95326178	95326179	*RBP4*	*RBP4*	0.22	0.51	2.40E-02	0.78
chr12	29376483	29376484	*FAR2*	*FAR2*	0.11	0.97	3.55E-02	0.74

3.6 | Validation of gene expression data

qRT-PCR analyses were performed to confirm the relative gene expression levels of genes significantly correlated with DNA methylation (*MITF*, *TERC*, *CDH13*, *PAX6*, *RHOB*, *HCK*, *NNMT*, *PMEL*, *EDNRB*, *ID4*, *EGFR*, *LEF1* and *ST8SIA1*). The qRT-PCR results were consistent with the microarray expression data, and robust correlation was observed in the majority of the tested transcripts ($0.74 \leq R \geq 1.00$; *P*-value ≤ .05). The relative expression levels are shown in Table S7.

4 | DISCUSSION

Invasion is a crucial step in metastasis formation in primary tumors including malignant melanoma. Recent advances in epigenome-wide DNA methylation methods have allowed for the identification of potential biomarkers that could be exploited in clinical settings.[15,43–47] However, in the case of early invasion steps in primary melanomas, insufficient data are available regarding the epigenetic mechanisms and especially the functionally relevant DNA methylation changes affecting gene expression patterns.

In the present work, we selected invasive cells in vitro from the original cell lines and analysed their invasion-associated DNA methylation changes, which followed by functional analysis of the observed changes at mRNA expression level. A number of studies have indicated that several tumor suppressor genes are silenced by DNA methylation in malignant melanoma compared with normal melanocytes or nevi, for example MITF gene.[15,48–50] MITF (microphthalmia-associated transcription factor) has been extensively studied in the context of master regulator of melanin production, suppression of invasion and regulation of the proliferative phenotype in melanoma

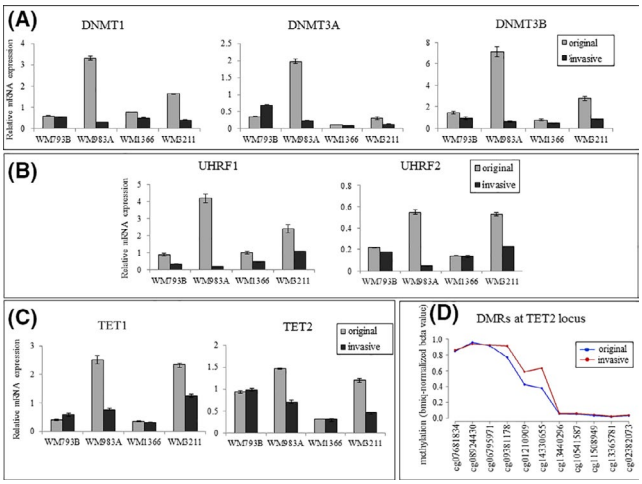

FIGURE 4 Analysis of relative expression levels of the original cell lines and the selected invasive cells by real-time quantitative PCR. Comparison of the relative mRNA expressions of (A) DNMTs, (B) UHRFs and (C) TETs in the original (WM793B, WM983A, WM1366 and WM3211) and the selected invasive melanoma cell lines (WM793B-INV, WM983A-INV, WM1366-INV and WM3211-INV). The data are presented as mean ± SD (three triplicates/samples). D, Line plot of significantly differentially methylated region at TET2 gene in the invasive (red line) and the original cell lines (blue line)

cells.[7,15,51,52] Its methylation change was also observed in melanoma brain metastases, suggesting its role not only in invasion property, but also in metastasis formation.[14,16] Selected invasive melanoma cells also showed hypermethylation of MITF that may directly affect MITF expression, giving a functional role of the detected epigenetic change.

Several studies have indicated that different biological behaviours of melanoma tumors are associated with distinct methylation subgroups.[14,18,53,54] The methylation changes in the *TFI2*, *HCK*, *MGMT* and *TP73* genes have been described in association with advanced clinical stage, shorter overall survival and the presence of metastasis, and it seems that, according to our results, these genes have a potential role in the earlier invasion steps of primary melanoma cells.[54–57]

In agreement with the widely accepted assumption that increased DNA methylation of certain promoters causes deregulation of the corresponding genes, we observed a negative correlation between the methylation and gene expression for several promoters such as *FBN1*, *ADORA2B* and *CHL1*. Hypermethylation was associated with the deregulation of fibrillin-1 (FBN1) that is a major component of microfibrils, and it can mediate cell adhesion in melanoma cells.[58] ADORA2B has been identified as specific receptor for 5'-methylthioadenosine (MTA) that can affect cell invasiveness in melanoma cells.[59] Neural cell adhesion molecule L1 (CHL1) is frequently down-regulated in different types of tumors, and it is verified to inhibit invasive growth and able to suppress further metastatic spread.[60] It seems that down-regulation of *CHL1* in association with methylation change was also observed in melanoma cells by Chatterjee et al[61] indicating that differentially methylated *CHL1* is a marked alteration in melanoma cells as well.

On the other hand, recent studies have shown that the methylation of the gene body is positively correlated with transcription.[45,62,63] Similar to these observations, hypermethylation in the gene body potentially plays a role in the up-regulation of *EGFR* and *RBP4* genes in the selected invasive cell populations. The role of EGFR in a range of neoplasms including melanoma is well known in association with tumor progression and metastasis.[64–66] Based on our results, methylation of *EGFR* gene body in correlation with up-regulated expression was revealed in the invasive cells. Epigenetic activation of *EGFR* upon resistant development to BRAF inhibitors has been previously described in melanoma, as well *EGFR* showed methylation difference in metastatic cell lines compared with its matched primary cell lines.[61,67] Recent studies indicated RBP4 serum levels as biomarker in colorectal cancer, and its overexpression was associated with ovarian cancer cell migration.[68–70] However, its function in melanoma has not been observed previously.

To obtain insights into the possible clinical relevance of the DNA methylation changes identified in our in vitro invasion model, we compared our results with the publicly available 450k TCGA-SKCM data sets. We identified several methylation changes that can have functional role in melanoma tumor samples, including HOXD13. In addition, we identified further eight differentially methylated members of the HOX gene family including *HOXA5*, *HOXB1*, *HOXB2*, *HOXB3*, *HOXB4*, *HOXC5*, *HOXC9* and *HOXD11*. Hypermethylation of homeobox genes is frequent in several cancers; however, this higher methylation is not consequently repress their downstream genes, as well as differentially methylated homeobox genes are not shown to be down-regulated in our invasive cells.[14,71–73] Differentially methylated HOXA5 and HOXD11 was found as a specific alteration in melanoma brain metastasis, and hypermethylation of HOXD9 was described in lymph node metastasis with poorer overall survival.[14,17,47] It is suggested that methylation pattern of homeobox genes can be specific to melanoma cells, and it is a possible approach to use epigenetic biomarker panels including homeobox genes in diagnosis, prediction and prognosis.[71,74]

The most interesting finding, between our results and the TCGA melanomas, is the hypermethylation of *ARHGAP22* and *NAV2* promoter regions that are commonly presented in locally invasive primary melanomas as well as during metastasis. Both NAV2 (neuron navigator 2) and ARHGAP22 have been identified to be involved in cell migration of different tumor types including melanoma.[75–77] NAV2 has several functional domains, which play key roles in the regulation of cytoskeletal remodelling and cell migration facilitating tumor invasion and metastasis.[78,79] Furthermore, a recent study suggested that NAV2 might contribute to melanoma invasion by epithelial-mesenchymal transition through the GSK-3β/β-catenin-SNAI2 pathway.[80] ARGHAP22 is a member of Rho GTPases that regulate the cytoskeleton-dependent processes during migration and invasion.[81] Silencing of ARHGAP22 results in increased number of elongated cells in melanoma cell lines and can regulate the mesenchymal-amoeboid transition.[82] The switch between mesenchymal and amoeboid types of movement allows metastatic tumor cells to adapt their morphology and movement in

different microenvironments.[82] Our results indicate the relevance of methylation-mediated gene expression changes in *ARHGAP22* and *NAV2* during the invasion of primary tumors and also during invasion-related melanoma progression.

Recent studies indicated that increased expression of UHRF1 and/or UHRF2 negatively regulates de novo DNA methylation, and their decreased expression has been observed to correlate with hypermethylation pattern in different tumors.[83,84] Consistent with the recent findings, both *UHRF1* and *UHRF2* genes showed down-regulation in invasive cells, and however, this mechanism need additional investigations.[61] Interestingly, the hypermethylation of *TET2* promoter region along with the down-regulation of gene was characteristic for the invasive melanoma cell population, which may contribute to the accumulation of 5mC and therefore plays a role in the global hypermethylation pattern of melanoma invasiveness; this observation need further investigations.

Overall, we found aberrant methylations of multiple genes in the selected invasive melanoma cells and a cohort of hypermethylated genes with decreased gene expression. Our results indicate the relevance of hypermethylated pattern in invasive melanoma cells, which might associated with the early invasion steps of melanoma.

ACKNOWLEDGEMENTS

We thank Florence Le Calvez-Kelm and Geoffroy Durand from IARC's Genetics Platform (GPS) and Fabienne Barbet from the ProfileXpert platform for the processing and scanning of the Illumina 450K arrays.

CONFLICT OF INTEREST

None declared.

AUTHOR CONTRIBUTIONS

MB, SE, VK and ZH conceived and designed the experiments. VK and IS performed invasion assay and RT-PCRs. SE, CC and NF performed methylation assays. SE and VL designed and analysed gene expression microarrays. SE and HH performed bioinformatics and statistical analyses. VK, ES, MB and RA written and reviewed the manuscript. All authors read and approved the final manuscript.

DATA AVAILABILITY STATEMENT

The data sets generated and/or analysed during the current study are available in the Gene Expression Omnibus (GEO) repository under accession number GSE114380 and GSE115852, http://www.ncbi.nlm.nih.gov/geo/query/acc.cgi?acc=GSE114380 and https://www.ncbi.nlm.nih.gov/geo/query/acc.cgi?acc=GSE115852.

ORCID

Margit Balázs https://orcid.org/0000-0002-4246-2321

REFERENCES

[1] C. M. Bailey, J. A. Morrison, P. M. Kulesa, *Pigment Cell Melanoma Res.* **2012**, *25*, 573.
[2] C. Bertolotto, *Scientifica* **2013**, *2013*, 635203.
[3] J. Paluncic, Z. Kovacevic, P. J. Jansson, D. Kalinowski, A. M. Merlot, M. L. Huang, H. C. Lok, S. Sahni, D. J. Lane, D. R. Richardson *Biochim. Biophys. Acta.* **1863**, *2016*, 770.
[4] F. van Zijl, G. Krupitza, W. Mikulits, *Mutat. Res.* **2011**, *728*, 23.
[5] S. Valastyan, R. A. Weinberg, *Cell* **2011**, *147*, 275.
[6] J. L. Orgaz, V. Sanz-Moreno, *Pigment Cell Melanoma Res.* **2013**, *26*, 39.
[7] A. Verfaillie, H. Imrichova, Z. K. Atak, M. Dewaele, F. Rambow, G. Hulselmans, V. Christiaens, D. Svetlichnyy, F. Luciani, L. Van den Mooter, S. Claerhout, M. Fiers, F. Journe, G. E. Ghanem, C. Herrmann, G. Halder, J. C. Marine, S. Aerts, *Nat. Commun.* **2015**, *6*, 6683.
[8] F. Nallet-Staub, V. Marsaud, L. Li, C. Gilbert, S. Dodier, V. Bataille, M. Sudol, M. Herlyn, A. Mauviel, *J. Invest. Dermatol.* **2014**, *134*, 123.
[9] I. M. Sanchez, A. E. Aplin, *J. Invest. Dermatol.* **2014**, *134*, 14.
[10] Y. Guo, J. Long, S. Lei, *J. Cell Physiol.* **2018**, *234*, 7356.
[11] Cancer Genome Atlas Network, *Cell* **2015**, *161*, 1681.
[12] M. Lauss, J. Nsengimana, J. Staaf, J. Newton-Bishop, G. Jonsson, *J. Invest. Dermatol.* **2016**, *136*, 2502.
[13] S. G. Jin, W. Xiong, X. Wu, L. Yang, G. P. Pfeifer, *Genomics* **2015**, *106*, 322.
[14] D. M. Marzese, R. A. Scolyer, J. L. Huynh, S. K. Huang, H. Hirose, K. K. Chong, E. Kiyohara, J. Wang, N. P. Kawas, N. C. Donovan, K. Hata, J. S. Wilmott, R. Murali, M. E. Buckland, B. Shivalingam, J. F. Thompson, D. L. Morton, D. F. Kelly, D. S. Hoon, *Hum. Mol. Genet.* **2014**, *23*, 226.
[15] M. Lauss, R. Haq, H. Cirenajwis, B. Phung, K. Harbst, J. Staaf, F. Rosengren, K. Holm, M. Aine, K. Jirstrom, A. Borg, C. Busch, J. Geisler, P. E. Lonning, M. Ringner, J. Howlin, D. E. Fisher, G. Jonsson, *J. Invest. Dermatol.* **2015**, *135*, 1820.
[16] E. S. de Araujo, D. T. Pramio, A. Y. Kashiwabara, P. C. Pennacchi, S. S. Maria-Engler, M. I. Achatz, A. H. Campos, J. P. Duprat, C. Rosenberg, D. M. Carraro, A. C. Krepischi, *Biomed. Res. Int.* **2015**, *2015*, 376423.
[17] A. Chatterjee, P. A. Stockwell, A. Ahn, E. J. Rodger, A. L. Leichter, M. R. Eccles, *Oncotarget* **2017**, *8*, 6085.
[18] P. F. Cheng, O. Shakhova, D. S. Widmer, O. M. Eichhoff, D. Zingg, S. C. Frommel, B. Belloni, M. I. Raaijmakers, S. M. Goldinger, R. Santoro, S. Hemmi, L. Sommer, R. Dummer, M. P. Levesque, *Genome Biol.* **2015**, *16*, 42.
[19] M. Bibikova, B. Barnes, C. Tsan, V. Ho, B. Klotzle, J. M. Le, D. Delano, L. Zhang, G. P. Schroth, K. L. Gunderson, J. B. Fan, R. Shen, *Genomics* **2011**, *98*, 288.
[20] P. Du, W. A. Kibbe, S. M. Lin, *Bioinformatics* **2008**, *24*, 1547.
[21] R. Pidsley, C. C. Y Wong, M. Volta, K. Lunnon, J. Mill, L. C. Schalkwyk, *BMC Genom.* **2013**, *14*, 293.
[22] M. J. Aryee, A. E. Jaffe, H. Corrada-Bravo, C. Ladd-Acosta, A. P. Feinberg, K. D. Hansen, R. A. Irizarry, *Bioinformatics* **2014**, *30*, 1363.
[23] Y. A. Chen, M. Lemire, S. Choufani, D. T. Butcher, D. Grafodatskaya, B. W. Zanke, S. Gallinger, T. J. Hudson, R. Weksberg, *Epigenetics* **2013**, *8*, 203.
[24] A. E. Teschendorff, F. Marabita, M. Lechner, T. Bartlett, J. Tegner, D. Gomez-Cabrero, S. Beck, *Bioinformatics* **2013**, *29*, 189.
[25] P. Du, X. Zhang, C. C. Huang, N. Jafari, W. A. Kibbe, L. Hou, S. M. Lin, *BMC Bioinformatics* **2010**, *11*, 587.
[26] G. K. Smyth, *Stat. Appl. Genet. Mol. Biol.* **2004**, *3*, Article3.
[27] T. J. Peters, M. J. Buckley, A. L. Statham, R. Pidsley, K. Samaras, R. V Lord, S. J. Clark, P. L. Molloy, *Epigenetics Chromatin* **2015**, *8*, 6.
[28] Triche, R package version 2.2.0., **2014**.

[29] N. Fernandez-Jimenez, A. Sklias, S. Ecsedi, V. Cahais, D. Degli-Esposti, A. Jay, P. B. Ancey, H. D. Woo, H. Hernandez-Vargas, Z. Herceg, *Epigenetics* **2017**, *12*, 964.
[30] T. C. Martin, I. Yet, P. C. Tsai, J. T. Bell, *BMC Bioinformatics* **2015**, *16*, 131.
[31] A. Colaprico, T. C. Silva, C. Olsen, L. Garofano, C. Cava, D. Garolini, T. S. Sabedot, T. M. Malta, S. M. Pagnotta, I. Castiglioni, M. Ceccarelli, G. Bontempi, H. Noushmehr, *Nucleic Acids Res.* **2016**, *44*, e71.
[32] A. Oghabian, D. Greco, M. J. Frilander, *BMC Bioinformatics* **2018**, *19*, 130.
[33] M. Lauss, M. Ringner, M. Hoglund, *Clin. Cancer Res.* **2010**, *16*, 4421.
[34] D. A. Mayes, Y. Hu, Y. Teng, E. Siegel, X. Wu, K. Panda, F. Tan, W. K. Yung, Y. H. Zhou, *Cancer Res.* **2006**, *66*, 9809.
[35] K. W. Hunter, R. Amin, S. Deasy, N. H. Ha, L. Wakefield, *Nat. Rev. Cancer* **2018**, *18*, 211.
[36] M. Werner-Klein, S. Scheitler, M. Hoffmann, I. Hodak, K. Dietz, P. Lehnert, V. Naimer, B. Polzer, S. Treitschke, C. Werno, A. Markiewicz, K. Weidele, Z. Czyz, U. Hohenleutner, C. Hafner, S. Haferkamp, M. Berneburg, P. Rummele, A. Ulmer, C. A. Klein, *Nat. Commun.* **2018**, *9*, 595.
[37] M. Tanaka, J. Shibahara, S. Ishikawa, T. Ushiku, T. Morikawa, A. Shinozaki-Ushiku, A. Hayashi, K. Misumi, A. Tanaka, H. Katoh, K. Sakuma, T. Kokudo, Y. Inagaki, J. Arita, Y. Sakamoto, K. Hasegawa, M. Fukayama, *Virchows Arch.* **2019**, *474*, 39.
[38] M. Fatemi, T. A. Paul, G. M. Brodeur, B. Shokrani, H. Brim, H. Ashktorab, *Cancer* **2014**, *120*, 172.
[39] X. Li, L. Huang, W. Gao, *Med. Sci. Monit.* **2019**, *25*, 771.
[40] G. Corda, G. Sala, R. Lattanzio, M. Iezzi, M. Sallese, G. Fragassi, A. Lamolinara, H. Mirza, D. Barcaroli, S. Ermler, E. Silva, H. Yasaei, R. F. Newbold, P. Vagnarelli, M. Mottolese, P. G. Natali, L. Perracchio, J. Quist, A. Grigoriadis, P. Marra, A. N. Tutt, M. Piantelli, S. Iacobelli, V. De Laurenzi, A. Sala, *J. Pathol.* **2017**, *241*, 350.
[41] P. He, S. Jiang, M. Ma, Y. Wang, R. Li, F. Fang, G. Tian, Z. Zhang, *Mol. Med. Rep.* **2015**, *12*, 503.
[42] W. C. Wei, W. C. Huang, Y. P. Lin, E. B. E. Becker, O. Ansorge, V. Flockerzi, D. Conti, G. Cenacchi, M. D. Glitsch, *J. Physiol.* **2017**, *595*, 5525.
[43] E. Fratta, L. Sigalotti, S. Coral, A. Covre, H. Nicolay, L. Pezzani, E. Cortini, F. Colizzi, E. Fonsatti, M. Altomonte, M. Maio, *Environ. Mol. Mutagen.* **2006**, *47*, 453.
[44] L. Sigalotti, E. Fratta, S. Coral, E. Cortini, A. Covre, H. J. M. Nicolay, L. Anzalone, L. Pezzani, A. M. Di Giacomo, E. Fonsatti, F. Colizzi, M. Altomonte, L. Calabro, M. Maio, *J. Cell Physiol.* **2007**, *212*, 330.
[45] L. Sigalotti, A. Covre, E. Fratta, G. Parisi, F. Colizzi, A. Rizzo, R. Danielli, H. J. Nicolay, S. Coral, M. Maio, *J. Transl. Med.* **2010**, *8*, 56.
[46] M. Maio, S. Coral, E. Fratta, M. Altomonte, L. Sigalotti, *Oncogene* **2003**, *22*, 6484.
[47] J. I. J. Orozco, T. A. Knijnenburg, A. O. Manughian-Peter, M. P. Salomon, G. Barkhoudarian, J. R. Jalas, J. S. Wilmott, P. Hothi, X. Wang, Y. Takasumi, M. E. Buckland, J. F. Thompson, G. V. Long, C. S. Cobbs, I. Shmulevich, D. F. Kelly, R. A. Scolyer, D. S. B. Hoon, D. M. Marzese, *Nat. Commun.* **2018**, *9*, 4627.
[48] V. F. Bonazzi, D. J. Nancarrow, M. S. Stark, R. J. Moser, G. M. Boyle, L. G. Aoude, C. Schmidt, N. K. Hayward, *PLoS ONE* **2011**, *6*, e26121.
[49] Y. Koga, M. Pelizzola, E. Cheng, M. Krauthammer, M. Sznol, S. Ariyan, D. Narayan, A. M. Molinaro, R. Halaban, S. M. Weissman, *Genome Res.* **2009**, *19*, 1462.
[50] K. Conway, S. N. Edmiston, Z. S. Khondker, P. A. Groben, X. Zhou, H. Chu, P. F. Kuan, H. Hao, C. Carson, M. Berwick, D. W. Olilla, N. E. Thomas, *Pigment Cell Melanoma Res.* **2011**, *24*, 352.
[51] E. Steingrimsson, N. G. Copeland, N. A. Jenkins, *Annu. Rev. Genet.* **2004**, *38*, 365.
[52] S. S. Dadras, R. J. Lin, G. Razavi, A. Kawakami, J. Du, E. Feige, D. A. Milner, M. F. Loda, S. R. Granter, M. Detmar, H. R. Widlund, M. A. Horstmann, D. E. Fisher, *Am. J. Pathol.* **2015**, *185*, 252.
[53] M. Lauss, M. Ringner, A. Karlsson, K. Harbst, C. Busch, J. Geisler, P. E. Lonning, J. Staaf, G. Jonsson, *BMC Med. Genomics* **2015**, *8*, 73.
[54] S. Ecsedi, H. Hernandez-Vargas, S. C. Lima, L. Vizkeleti, R. Toth, V. Lazar, V. Koroknai, T. Kiss, G. Emri, Z. Herceg, R. Adany, M. Balazs, *PLoS ONE* **2014**, *9*, e96612.
[55] C. Lo Nigro, H. Wang, A. McHugh, L. Lattanzio, R. Matin, C. Harwood, N. Syed, E. Hatzimichael, E. Briasoulis, M. Merlano, A. Evans, A. Thompson, I. Leigh, C. Fleming, G. J. Inman, C. Proby, T. Crook, *J. Invest. Dermatol.* **2013**, *133*, 1278.
[56] G. Micevic, N. Theodosakis, M. Bosenberg, *Clin. Epigenetics* **2017**, *9*, 34.
[57] R. Tuominen, R. Jewell, J. J. van den Oord, P. Wolter, U. Stierner, C. Lindholm, C. Hertzman Johansson, D. Linden, H. Johansson, M. Frostvik Stolt, C. Walker, H. Snowden, J. Newton-Bishop, J. Hansson, S. Egyhazi Brage, *Int. J. Cancer* **2015**, *136*, 2844.
[58] D. V. Bax, S. E. Bernard, A. Lomas, A. Morgan, J. Humphries, C. A. Shuttleworth, M. J. Humphries, C. M. Kielty, *J. Biol. Chem.* **2003**, *278*, 34605.
[59] K. Limm, S. Wallner, V. M. Milenkovic, C. H. Wetzel, A. K. Bosserhoff, *Eur. J. Cancer* **2014**, *50*, 2714.
[60] V. N. Senchenko, G. S. Krasnov, A. A. Dmitriev, A. V. Kudryavtseva, E. A. Anedchenko, E. A. Braga IV, T. T. Kondratieva Pronina, S. V. Ivanov, E. R. Zabarovsky, M. I. Lerman, *PLoS ONE* **2011**, *6*, e15612.
[61] A. Chatterjee, E. J. Rodger, A. Ahn, P. A. Stockwell, M. Parry, J. Motwani, S. J. Gallagher, E. Shklovskaya, J. Tiffen, M. R. Eccles, P. Hersey, *iScience*, **2018**, *4*, 312.
[62] D. Sarkar, E. Y. Leung, B. C. Baguley, G. J. Finlay, M. E. Askarian-Amiri, *Epigenetics* **2015**, *10*, 103.
[63] R. Lister, M. Pelizzola, R. H. Dowen, R. D. Hawkins, G. Hon, J. Tonti-Filippini, J. R. Nery, L. Lee, Z. Ye, Q. M. Ngo, L. Edsall, J. Antosiewicz-Bourget, R. Stewart, V. Ruotti, A. H. Millar, J. A. Thomson, B. Ren, J. R. Ecker, *Nature* **2009**, *462*, 315.
[64] J. M. Haydn, A. Hufnagel, J. Grimm, K. Maurus, M. Schartl, S. Meierjohann, *Oncotarget* **2014**, *5*, 5040.
[65] P. Uribe, S. Gonzalez, *Pathol. Res. Pract.* **2011**, *207*, 337.
[66] Z. Rakosy, L. Vizkeleti, S. Ecsedi, Z. Voko, A. Begany, M. Barok, Z. Krekk, M. Gallai, Z. Szentirmay, R. Adany, M. Balazs, *Int. J. Cancer* **2007**, *121*, 1729.
[67] J. Wang, S. K. Huang, D. M. Marzese, S. C. Hsu, N. P. Kawas, K. K. Chong, G. V. Long, A. M. Menzies, R. A. Scolyer, S. Izraely, O. Sagi-Assif, I. P. Witz, D. S. B. Hoon, *J. Invest. Dermatol.* **2015**, *135*, 532.
[68] P. Raghu, B. Sivakumar, *Biochim. Biophys. Acta* **2004**, *1703*, 1.
[69] W. Fei, L. Chen, J. Chen, Q. Shi, L. Zhang, S. Liu, L. Li, L. Zheng, X. Hu, *Oncotarget* **2017**, *8*, 92254.
[70] Y. Wang, Z. Zhang, *J. Ovarian Res.* **2018**, *11*, 29.
[71] J. Furuta, Y. Nobeyama, Y. Umebayashi, F. Otsuka, K. Kikuchi, T. Ushijima, *Cancer Res.* **2006**, *66*, 6080.
[72] T. A. Rauch, Z. Wang, X. Wu, K. H. Kernstine, A. D. Riggs, G. P. Pfeifer, *Tumour Biol.* **2012**, *33*, 287.
[73] S. Tommasi, D. L. Karm, X. Wu, Y. Yen, G. P. Pfeifer, *Breast Cancer Res.* **2009**, *11*, R14.
[74] M. F. Rodrigues, C. M. Esteves, F. C. Xavier, F. D. Nunes, *Genomics* **2016**, *108*, 185.
[75] T. Maes, A. Barcelo, C. Buesa, *Genomics* **2002**, *80*, 21.
[76] S. Alinezhad, R. M. Vaananen, J. Mattsson, Y. Li, T. Tallgren, N. Tong Ochoa, A. Bjartell, M. Akerfelt, P. Taimen, P. J. Bostrom, K. Pettersson, M. Nees, *PLoS ONE* **2016**, *11*, e0155901.
[77] S. Liu, Y. Wang, W. Xue, H. Liu, Y. Xu, Q. Shi, W. Wu, D. Zhu, C. I. Amos, S. Fang, J. E. Lee, T. Hyslop, Y. Li, J. Han, Q. Wei, *Int. J. Cancer* **2017**, *141*, 721.
[78] E. G. Stringham, K. L. Schmidt, *Cell Adh. Migr.* **2009**, *3*, 342.
[79] F. Tan, H. Zhu, Y. Tao, N. Yu, Q. Pei, H. Liu, Y. Zhou, H. Xu, X. Song, Y. Li, Z. Zhou, X. He, X. Zhang, H. Pei, *J. Exp. Clin. Cancer Res.* **2015**, *34*, 117.

[80] W. Hu, X. Li, R. Cheng, J. Ke, Y. Liu, M. Ma, Y. Cao, D. Liu, *Arch Dermatol. Res.* **2019**, *311*, 399.
[81] K. Pankova, D. Rosel, M. Novotny, J. Brabek, *Cell Mol. Life Sci.* **2010**, *67*, 63.
[82] V. Sanz-Moreno, G. Gadea, J. Ahn, H. Paterson, P. Marra, S. Pinner, E. Sahai, C. J. Marshall, *Cell* **2008**, *135*, 510.
[83] Y. Jia, P. Li, L. Fang, H. Zhu, L. Xu, H. Cheng, J. Zhang, F. Li, Y. Feng, Y. Li, J. Li, R. Wang, J. X. Du, T. Chen, H. Ji, J. Han, W. Yu, Q. Wu, J. Wong, *Cell Discov.* **2016**, *2*, 16007.
[84] H. Lu, S. Bhoopatiraju, H. Wang, N. P. Schmitz, X. Wang, M. J. Freeman, C. L. Forster, M. R. Verneris, M. A. Linden, T. C. Hallstrom, *Oncotarget* **2016**, *7*, 76047.

SUPPORTING INFORMATION

Additional supporting information may be found online in the Supporting Information section.

Figure S1. Visualization of DNA co-methylation patterns at CpG shores in invasive melanoma cell lines. Co-methylation plots show the *P* values of the methylation difference between the selected invasive (WM793B-INV, WM983A-INV, WM1366-INV, and WM3211-INV) and the original cell lines (WM793B, WM983A, WM1366, and WM3211) for differentiallym ethylated regions (DMRs).The referencep robe is highlighted in black, the rest of the circles are marked according to Spearman correlation coefficients among probes. Blue and the violet lines represent the methylation level of the invasive and original cell lines, respectively.The green horizontal line shows the position of CpG island of theregion

Table S1. Primer sequences used in RT-qPCR experiments

Table S2. Significant differencially methylated regions (DMRs) in selected invasive population compared to the original cell lines

Table S3. Differentially methylated probes (DMPs) corresponding to significant DMRs in selected invasive population compared to the original cell lines

Table S4. Enrichment analysis of the related genes of significant hypermethylated DMPs meeting the criteria of mean $\Delta\beta > 0.1$

Table S5. Significant correlation between differencially methylated probes (DMPs) and gene expression data

Table S6. Differencially methylated probes (DMPs) corresponding to significant DMRs in Clark stage-5 primary tumours compared to lower than stage-5 primary melanomas

Table S7. Relative† mRNA expression in the original and the selected invasive cell lines

Methods S1. Genome wide DNA methylation analysis

How to cite this article: Koroknai V, Szász I, Hernandez-Vargas H, et al. DNA hypermethylation is associated with invasive phenotype of malignant melanoma. *Exp Dermatol*. 2019;00:1–10. https://doi.org/10.1111/exd.14047